

Excitation functions for (p, n) reactions on ^{79}Br and $^{127}\text{I}^\dagger$

R. Collé and R. Kishore

Chemistry Department, Brookhaven National Laboratory, Upton, New York 11973

(Received 17 January 1974)

Excitation functions for the $^{79}\text{Br}(p, n)^{79}\text{Kr}$ and $^{127}\text{I}(p, n)^{127}\text{Xe}$ reactions have been determined from 3 to 25 MeV by the activation method. KBr and KI targets of natural isotopic abundances were encapsulated in Mylar to prevent escape of the gaseous ^{79}Kr and ^{127}Xe . Disintegration rates were obtained by assaying selected γ rays with calibrated Ge(Li) detectors; beam intensities were determined with a Faraday cup. The measured absolute cross sections have uncertainties of less than 10% with energy uncertainties of $\lesssim 100$ keV. The excitation functions are compared to Monte Carlo calculations based on an intranuclear-cascade statistical-evaporation model.

[NUCLEAR REACTIONS $^{79}\text{Br}(p, n)^{79}\text{Kr}$ and $^{127}\text{I}(p, n)^{127}\text{Xe}$, $E = 3\text{--}25$ MeV; measured $\sigma(E)$. Natural targets, Ge(Li) detector.]

I. INTRODUCTION

The present investigation is part of a study in this laboratory of the excitation functions for various (p, n) reactions from 3 to 25 MeV.¹ Such data are useful for comparison to theoretical models; in addition excitation functions for production of noble gas nuclides are of application in nuclear medicine.² These reactions have not been studied in detail³⁻⁸ and only very few cross sections have been reported.^{4,7,8} This may be due to the experimentally unpleasant combination of halogen targets and rare gas product nuclei which is not very amenable to the usual technique of stacked foil activation. All of the published^{4,7,8} cross sections were determined by assaying the rare gas product activity. Humes *et al.*⁷ and Blosser and Handley⁴ measured $^{79}\text{Br}(p, n)^{79}\text{Kr}$ reaction cross sections at 6.75 and 12 MeV, respectively. The latter authors used an intimate mixture of NaBr and CuO to determine the $^{79}\text{Br}(p, n)^{79}\text{Kr}$ cross section relative to the $^{63}\text{Cu}(p, n)^{63}\text{Zn}$ cross section measured by Ghoshal.⁹ Both groups^{4,7} failed to consider (or neglected to report) the possibility of loss of ^{79}Kr gas from the targets. Narang and Yaffe,⁸ using encapsulated CuI targets, measured 11 cross sections for the $^{127}\text{I}(p, n)^{127}\text{Xe}$ reaction in the energy range from 7 to 63 MeV. These measurements were made relative to the $^{63}\text{Cu}(p, n)^{63}\text{Zn}$ and $^{65}\text{Cu}(p, pn)^{64}\text{Cu}$ monitor reactions.^{9,10} Although adequate precautions were taken against loss of the ^{127}Xe gas, this study was limited by an energy uncertainty which was estimated to be no better than ± 2 MeV.

II. EXPERIMENTAL TECHNIQUES

The excitation functions were measured with proton beams from the Brookhaven tandem Van de

Graaff accelerators. Typically, the irradiations were of 30-min duration and were performed with average beam currents of 100–300 nA. Specific details of the experimental techniques have been reported previously.¹ The proton beam was diffused after energy analysis to provide a large beam spot which was then collimated to 1 cm diam. The beam currents were measured with a Faraday cup and current integrator. The cup had provision for magnetic suppression of secondary electrons produced at the collimator. The accuracy of the current integration was estimated to be $\approx 1\%$. Energy degradation of the beam in passing through the absorbers (window, small air path, and Mylar target cover) and target was calculated¹ from the stopping power tabulations of Northcliffe and Schilling¹¹ and Williamson, Boujot, and Picard.¹² Mean energies for the irradiations were taken as the proton energies at the target centers. Errors in the mean energies which amounted to ≈ 100 keV were obtained by quadratic propagation of the uncertainties of the incident beam energies, the errors in the energy losses for each absorber and target, and the energy straggling¹ for each absorber and target. Target thickness ranged from ≈ 100 keV at 3 MeV to ≈ 25 keV at 25 MeV. These target thicknesses were sufficiently small so that even in the worst cases, the corrections for energy resolution were negligible ($< 1\%$).

The targets of bromine and iodine have been previously described.¹³ They consisted of thin ($\approx 2\text{--}3\text{ mg/cm}^2$) uniform films of either KBr or KI (natural isotopic abundances) vacuum evaporated onto high-purity aluminum which were subsequently encapsulated in vacuum between two sheets of $\approx 12\text{--}15\text{ mg/cm}^2$ heat-sealable Mylar. This encapsulation was shown¹³ to quantitatively retain the radioactive

product gases (⁷⁹Kr or ¹²⁷Xe) over the entire measurement period. Target thicknesses were determined to 2–4% both by weighing targets having known areas of deposition and by chemical analyses following the irradiations and counting measurements. Differences between thicknesses determined by weighing and that by chemical determination were usually <1% for the KBr targets and typically 1–3% for the KI targets.

After irradiation, absolute disintegration rates of the ⁷⁹Kr or ¹²⁷Xe product nuclei in the encapsulated targets were determined by measuring their γ rays with calibrated¹³ 4096-channel Ge(Li) spectrometers. Copper absorbers (≈ 370 mg/cm²) were placed over the targets during counting to annihilate positrons at the sources and to attenuate the x rays in order to minimize coincident summing with γ rays. Each target was assayed at least several times over a period of 1–4 half-lives. Analysis of the γ -ray spectra was performed by means of a modified version of the BRUTAL¹⁴ computer code. The resultant γ -ray decay curves were then fitted to the known half-lives (see Table I) with the least-squares CLSQ¹⁵ program. After applying the detector efficiencies and correcting for absorption (in both the source and Cu absorber) and coincident summing (with coincident γ rays, x rays, and annihilation radiation), the γ -ray emission rates were converted to absolute disintegration rates by the use of the known γ -ray abundances (see Table I).

The principal radioactive decay characteristics of ⁷⁹Kr and ¹²⁷Xe which were used in this work are provided in Table I. Disintegration rates were obtained by averaging the results from the three γ rays in ⁷⁹Kr and the four in ¹²⁷Xe. In this way, the values of the cross sections are less subject to possible systematic errors (such as in the γ -ray abundances or detection efficiencies). The uncertainties in the cross sections are in the range 6–9% and were obtained by quadratically summing

TABLE I. Radioactive decay characteristics (Ref. 13) of the product nuclei which were used for the cross-section measurements in this work.

Product nucleus	Half-life	γ -ray energy (keV)	γ -ray abundance (photons/100 disintegrations)
⁷⁹ Kr	35.04 \pm 0.05 h	261.3	12.7 \pm 0.4
		397.5	9.5 \pm 0.3
		606.1	8.1 \pm 0.2
¹²⁷ Xe	36.3 \pm 0.3 day	145.2	4.24 \pm 0.21
		172.1	24.7 \pm 1.0
		202.8	68.1 \pm 1.3
		375.0	17.4 \pm 1.0

TABLE II. Experimental activation cross sections as a function of proton energy for the reaction ⁷⁹Br(*p*, *n*) - ⁷⁹Kr.^a

Proton energy (MeV)	Cross section (mb)	Proton energy (MeV)	Cross section (mb)
3.00	1.29 \pm 0.14	10.98	725 \pm 52
4.33	52.2 \pm 4.0	12.13	646 \pm 46
5.55	160 \pm 12	13.07	522 \pm 38
6.70	328 \pm 21	13.12	535 \pm 38
7.13	394 \pm 27	13.17	506 \pm 37
7.76	442 \pm 34	14.11	434 \pm 32
8.75	563 \pm 37	16.69	158 \pm 12
8.80	526 \pm 47	19.76	63.9 \pm 4.9
8.93	547 \pm 38	21.29	51.0 \pm 4.2 ^a
9.92	626 \pm 44	23.30	94.4 \pm 7.1 ^a
9.92	626 \pm 46	24.82	204 \pm 17 ^a
10.98	723 \pm 52		

^a ⁸¹Br(*p*, 3*n*)⁷⁹Kr contributes above its reaction threshold (20.71 MeV); apparent cross section is

$$\sigma = \sigma[{}^{79}\text{Br}(p, n)] + \frac{N({}^{81}\text{Br})}{N({}^{79}\text{Br})} \sigma[{}^{81}\text{Br}(p, 3n)].$$

the contributions from peak analyses (including counting statistics) and decay curve analyses (<3%), absolute detection efficiencies (5–10%), γ -ray abundances (2–5%), target thicknesses (2–4%), and current integration ($\approx 1\%$).

III. RESULTS AND DISCUSSION

The results of the present cross-section measurements are tabulated in Table II for ⁷⁹Kr and in Table III for ¹²⁷Xe and have been plotted as excitation functions in Figs. 1 and 2 (shown as filled circles). The figures also contain (as open cir-

TABLE III. Experimental activation cross section for the reaction ¹²⁷I(*p*, *n*)¹²⁷Xe as a function of proton energy.

Proton energy (MeV)	Cross section (mb)	Proton energy (MeV)	Cross section (mb)
3.01	0.081 \pm 0.011	10.98	385 \pm 29
4.34	1.61 \pm 0.13	10.98	402 \pm 35
5.56	20.3 \pm 1.6	12.13	305 \pm 24
6.70	86.3 \pm 7.4	13.12	193 \pm 18
7.14	135 \pm 12	13.17	193 \pm 17
7.77	194 \pm 17	14.12	134 \pm 11
7.77	198 \pm 15	15.16	92.1 \pm 7.6
8.76	362 \pm 32	16.69	62.5 \pm 5.3
8.79	362 \pm 29	18.23	47.8 \pm 4.2
8.93	375 \pm 31	19.77	42.9 \pm 3.6
9.92	443 \pm 33	21.29	34.9 \pm 2.9
9.92	471 \pm 40	23.30	32.5 \pm 2.8
10.98	365 \pm 31	24.82	30.2 \pm 2.7

cles) the results of Blosser and Handley⁴ and Humes *et al.*⁷ for ^{79}Kr , and the results of Narang and Yaffe⁸ for ^{127}Xe .

For the $^{79}\text{Br}(p,n)^{79}\text{Kr}$ reaction (Fig. 1), the two previously reported values are 86 ± 5 mb at 6.75 MeV⁷ and 1050 ± 350 mb at 12 MeV.⁴ The former value is lower than that of the present work by almost a factor of 4. This is most probably due to loss of gaseous ^{79}Kr activity from their target. The measurement at 12 MeV by Blosser and Handley⁴ was based on Ghoshal's⁹ value of 530 mb for the $^{63}\text{Cu}(p,n)^{63}\text{Zn}$ monitor reaction cross section. Ghoshal's cross sections in this energy region have recently been shown to be too high by $\approx 20\%$; the new measurement¹ at 12 MeV is 450 mb. If one corrects their⁴ original value by the ratio 450/530, the renormalized cross section, 890 ± 300 mb (which is plotted in Fig. 1) is in reasonable agreement with the present results. Above 20 MeV, the excitation function shown in Fig. 1 consists of the

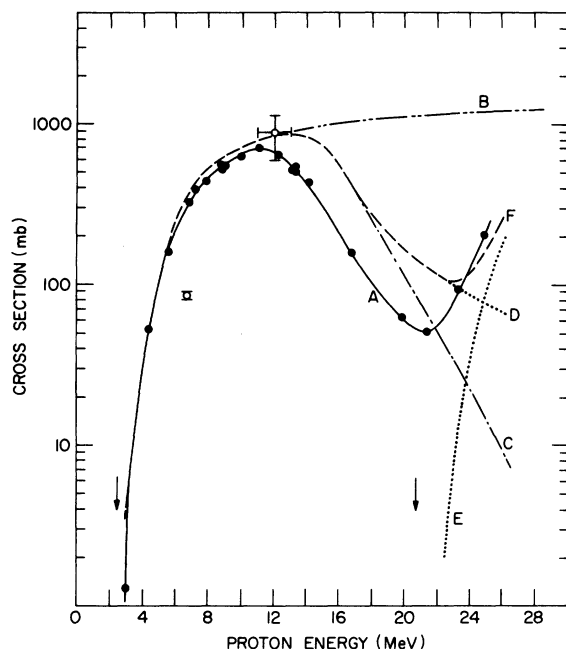


FIG. 1. Experimental excitation function for the $^{79}\text{Br}(p,n)^{79}\text{Kr} + ^{81}\text{Br}(p,3n)^{79}\text{Kr}$ reactions and comparison with evaporation and cascade-evaporation calculations. The filled circles represent the present work and the open circles show results from previous measurements (Refs. 4 and 7). The labeled curves are: A, smooth curve through experimental points; B, optical-model reaction cross sections taken from Ref. 22; C, DFF evaporation calculations for $^{79}\text{Br}(p,n)$; D, VEGAS-DFF cascade-evaporation calculations for $^{79}\text{Br}(p,n)$; E, VEGAS-DFF cascade-evaporation calculations for $^{81}\text{Br}(p,3n)$; F, weighted sum of curves D and E. The (p,n) and $(p,3n)$ reaction thresholds at 2.45 and 20.7 MeV, respectively, are labeled with arrows.

weighted sum of the $^{79}\text{Br}(p,n)^{79}\text{Kr}$ and $^{81}\text{Br}(p,3n)^{79}\text{Kr}$ reaction cross sections. The thresholds for these reactions (labeled in the figure with arrows) are 2.45 and 20.7 MeV, respectively.

The peak position for the $^{127}\text{I}(p,n)^{127}\text{Xe}$ reaction (Fig. 2) was estimated by Narang and Yaffe⁸ to be at 15 ± 2 MeV. In comparison to the present results, this appears to be in error by ≈ 5 MeV; however their peak cross section (≈ 450 mb) is in good agreement. At energies above the peak, their cross sections decrease much more rapidly than the present data. Their cross section at 25 MeV is lower by approximately a factor of 3. Absolute disintegration rates were determined in their work⁸ by assaying the 375-keV γ ray and assuming 20.7 photons per 100 disintegrations. Therefore, for comparison to the present results, their values should be increased by a factor of 1.19 to remove the systematic differences due to the assumed decay characteristics (see Table I). In addition, their cross sections were determined relative to the $^{63}\text{Cu}(p,n)^{63}\text{Zn}$ and $^{65}\text{Cu}(p,pn)^{64}\text{Cu}$ reaction cross sections.^{9,10} The values they used for these

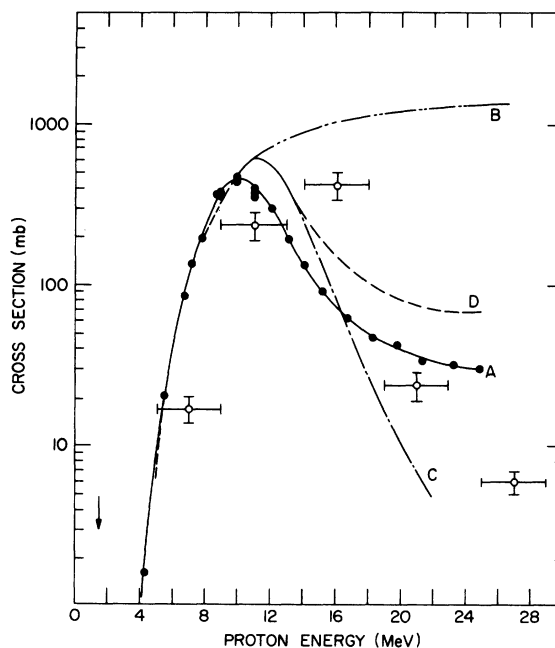


FIG. 2. Experimental excitation function for the $^{127}\text{I}(p,n)^{127}\text{Xe}$ reaction and comparison with evaporation and cascade-evaporation calculations. The filled circles represent the present work and the open circles show results from Ref. 8. The labeled curves are: A, smooth curve through experimental points; B, optical-model reaction cross sections taken from Ref. 22; C, DFF evaporation calculations; D, VEGAS-DFF cascade-evaporation calculations. The reaction threshold at 1.46 MeV is labeled with an arrow.

monitor reaction cross sections do not withstand careful scrutiny. For example, their low-energy cross sections which are relative to the $^{63}\text{Cu}(p, n)^{63}\text{Zn}$ reaction can be in error by over 30% as indicated by the recent measurements and compilation of Ref. 1. Similarly, the anomalously large cross section at 16 MeV may be reflecting a large error in the $^{65}\text{Cu}(p, pn)^{64}\text{Cu}$ monitor reaction cross section. At 16 MeV, the cross sections for this latter reaction are rapidly increasing and thus are subject to considerable errors. Reliable data for this reaction below 25 MeV are rather scarce.¹⁰

In Figs. 1 and 2, the experimental excitation functions are compared to Monte Carlo calculations based on an intranuclear-cascade statistical-evaporation model.¹⁶⁻¹⁹ The calculations were performed as previously described¹ with the STEPNO version (with improved nucleon density distribution as discussed in Ref. 17) of the VEGAS code of Chen *et al.*¹⁶ for the cascade stage followed by the DFF code of Dostrovsky, Fraenkel, and Friedlander¹⁹ for the evaporation stage. Pure compound-nucleus statistical-evaporation calculations were also made with the DFF code. The fractional production probabilities (i.e., probability for production of a given product nucleus per incident proton) from both the simple evaporation and cascade-evaporation calculations were converted to production cross sections using the optical-model reaction cross sections of Mani, Melkanoff, and Iori.²⁰ The calculated results are provided in Figs. 1 and 2. The curves identified by B, C, and D are, respectively, the optical-model reaction cross sections taken from Ref. 20, the DFF evaporation calculations, and the VEGAS-DFF cascade-evaporation calculations. Figure 1 also contains VEGAS-DFF cascade-evaporation calculations for the $^{81}\text{Br}(p, 3n)^{79}\text{Kr}$ reaction excitation function (curve E). The weighted sum of the $^{79}\text{Br}(p, n)^{79}\text{Kr}$ and $^{81}\text{Br}(p, 3n)^{79}\text{Kr}$ reaction cross sections is labeled in the figure as curve F. The qualitative features of similar calculations have been described in several previous reports.^{1, 21-23} In comparison to the present experimental results, the general shapes of the excitation functions are well reproduced by the cascade-

evaporation calculations. However, in general, peak positions are predicted to be ≈ 1.5 – 3.0 MeV higher than the experimental values, and the calculations overestimate the experimental cross sections on the higher-energy side of the peaks. Similar trends have been described¹ previously and perhaps it would be useful to recapitulate the reason for the disagreement at the higher energies (>11 MeV). It can be related to an overestimation of the fraction of events which proceed through direct processes. In the present cases, this fraction increases from $\approx 12\%$ at 13 MeV to $\approx 68\%$ at 25 MeV for the $^{79}\text{Br}(p, n)^{79}\text{Kr}$ reaction, and from $\approx 12\%$ at 11 MeV to over 90% at 25 MeV for the $^{127}\text{I}(p, n)^{127}\text{Xe}$ reaction. The antithesis of this effect was observed in the STEP version of the VEGAS-DFF calculations^{21, 22} which included provision for reflection and refraction of cascade nucleons at the boundaries of the changing potential in the assumed nuclear density step distribution. Simplistically, this reflection and refraction has the effect of trapping the nucleons and thereby enhancing compound-nucleus formation. When it is absent, compound-nucleus formation decreases in favor of direct processes which lead to the reaction products. In conclusion, the STEPNO version of the calculations (present work) appears to be characterized by an overestimation of direct interaction, while in the STEP calculation compound-nucleus formation is overestimated.

ACKNOWLEDGMENTS

The authors would like to thank J. B. Cumming and S. Katcoff for valuable discussions throughout the course of this work and for their thoughtful criticism of this manuscript during its preparation. They would also like to thank G. Harp for help in carrying out the VEGAS and DFF calculations and for discussions of the calculations. Assistance provided by E. Ritter and R. Becker in preparing the targets, R. W. Stoenner and E. Norton in performing the bromine and iodine chemical analyses, and D. E. Alburger and staff of the Brookhaven tandem Van de Graaff accelerators in obtaining irradiations is gratefully acknowledged.

[†]Research supported by Advanced Research Projects Agency (ARPA order No. 1590) and the U. S. Atomic Energy Commission.

¹R. Collé, R. Kishore, and J. B. Cumming, *Phys. Rev. C* **9**, 1819 (1974).

²H. N. Wagner, Jr., *Principles of Nuclear Medicine* (Saunders, Philadelphia, 1968), p. 293; P. B. Hoffer, P. V. Harper, R. N. Beck, V. Stark, H. Krizek,

L. Heck, and N. Lembares, *J. Nucl. Medicine* **14**, 172 (1973).

³F. Boehm, P. Marmier, and P. Preiswerk, *Helv. Phys. Acta* **25**, 599 (1952).

⁴H. G. Blosser and T. H. Handley, *Phys. Rev.* **100**, 1340 (1955).

⁵G. A. Jones, *Nucl. Phys.* **12**, 167 (1958).

⁶C. H. Johnson, A. Galonsky, and C. N. Inskeep, Oak

- Ridge National Laboratory Report No. ORNL-2910, 1960 (unpublished), p. 25.
- ⁷R. M. Humes, G. F. Dell, Jr., W. D. Ploughe, and H. J. Hausman, *Phys. Rev.* **130**, 1522 (1963).
- ⁸V. P. Narang and L. Yaffe, *Can. J. Chem.* **46**, 3171 (1968).
- ⁹S. N. Ghoshal, *Phys. Rev.* **80**, 939 (1950).
- ¹⁰The absolute cross sections for the $^{65}\text{Cu}(p,pn)^{64}\text{Cu}$ monitor reaction used by Narang and Yaffe (Ref. 8) were taken from an unpublished study by S. Meghir (Ph. D. thesis, McGill University, Montreal, Quebec, 1962). This same laboratory has recently remeasured these monitor cross sections; D. A. Newton, S. Sarkar, L. Yaffe, and R. B. Moore, *J. Inorg. Nucl. Chem.* **35**, 361 (1973).
- ¹¹L. C. Northcliffe and R. F. Schilling, *Nucl. Data A* **7**, 223 (1970).
- ¹²C. F. Williamson, J. P. Boujot, and J. Picard, Centre d'Etudes Nucléaires de Saclay Report No. CEA-R3042, 1966 (unpublished).
- ¹³R. Collé and R. Kishore, *Phys. Rev. C* **9**, 981 (1974).
- ¹⁴R. Gunnink, H. B. Levy, and J. B. Niday, University of California Radiation Laboratory Report No. UCID-15140 (unpublished); modified by B. R. Erdal (unpublished).
- ¹⁵J. B. Cumming, National Academy of Sciences-National Research Council, Nuclear Science Series Report No. NAS-NS-3107, 1962 (unpublished).
- ¹⁶K. Chen, Z. Fraenkel, G. Friedlander, J. R. Grover, J. M. Miller, and Y. Shimamoto, *Phys. Rev.* **166**, 949 (1968).
- ¹⁷K. Chen, G. Friedlander, and J. M. Miller, *Phys. Rev.* **176**, 1208 (1968).
- ¹⁸K. Chen, G. Friedlander, G. D. Harp, and J. M. Miller, *Phys. Rev. C* **4**, 2234 (1971).
- ¹⁹I. Dostrovsky, Z. Fraenkel, and G. Friedlander, *Phys. Rev.* **116**, 683 (1959).
- ²⁰G. S. Mani, M. A. Melkanoff, and I. Iori, Centre d'Etudes Nucléaires de Saclay Report No. CEA-2379, 1963 (unpublished).
- ²¹G. B. Saha, N. T. Porile, and L. Yaffe, *Phys. Rev.* **144**, 962 (1966).
- ²²D. R. Sachdev, N. T. Porile, and L. Yaffe, *Can. J. Chem.* **45**, 1149 (1967).
- ²³J. J. Hogan, *Phys. Rev. C* **6**, 810 (1972).